Chemical Physics Letters 778 (2021) 138817

Contents lists available at ScienceDirect

Chemical Physics Letters

journal homepage: www.elsevier.com/locate/cplett

Research paper

Electromechanical response of lamellar forming ionic diblock copolymer thin films

Mengze Ma [a,c], Yao Fu [b,*]

[a] Department of Aerospace Engineering and Engineering Mechanics, University of Cincinnati, Cincinnati, OH 45221, United States
[b] Department of Aerospace and Ocean Engineering, Virginia Tech, Blacksburg, VA 24061, United States
[c] The First Affiliated Hospital of Zhengzhou University, Zhengzhou, Henan 450052, PR China

ARTICLE INFO

Keywords:
Ionic block copolymers
Thin film
Electric field
Molecular dynamics

ABSTRACT

Electromechanical responses of lamellar forming neutral-charged diblock copolymers (BCPs) in thin films are investigated using coarse-grained molecular dynamics simulations, where the electric permittivity of polymer monomer is described by explicitly introducing freely rotating dipoles. Effects of an applied electric field on the ion transport, morphological change and stress build-up are studied in detail. In particular, we focus on the responses to strong electric fields in terms of the ion dissociation and stress distribution along the film thickness. The different stages of BCP evolution under the electric field are characterized. This work paves a way towards establishing a modeling scheme that describes the response of ionic polymers in the presence of applied electric field.

1. Introduction

Microphase separation in neutral block copolymers (BCPs) has received tremendous attention over the last five decades [1–17]. Thermodynamic properties of the microphase separation are dictated by the interplay of entropic penalty due to chain stretching and repulsive interactions among the monomers of different types in the block copolymers. Despite this simple picture from the thermodynamics aspect, chain dynamics in microphase separated morphologies is quite complicated due to the inhomogeneous density profiles. In addition, for various applications requiring electrical responses from polymers [18–22], ionic blocks have been routinely linked to a neutral block so that the ionic block provides the necessary electrical response and the neutral block provides the requisite other property such as the mechanical strength [23–25]. Block copolymers are thus also considered as promising smart materials. In the last decade, several theoretical and experimental studies have focused on understanding the thermodynamics of microphase separation in ionic block copolymers [26–34]. These studies have established the entropic and enthalpic effects of counterions [4,35,36]. The entropic effects tend to stabilize the disordered phase and the enthalpic effects resulting from the interaction of ions with the polar groups of the polymers tend to stabilize microphase separated morphologies.

Despite the developments in the area of thermodynamics, the understanding in the kinetics of ionic block copolymers under the electric field is still in infancy stage. Seminal works by Amundson and Helfand [37,38] have laid out the foundation on the effects of applied electric field on the neutral diblock copolymers. In the last decade, researchers have explored the effects of counterions on the threshold voltage required for the morphological transformation in the presence of applied electric fields [27,28]. Most of these studies have focused on the equilibrium conditions without considering the kinetics of the morphological transformations. These studies have clearly pointed out the importance of dielectric contrast among the microphase separated domains and the concentration of counterions in affecting the threshold electric field required to incite morphological changes.

In this study, we have used coarse-grained molecular dynamics simulations (CGMD) to explore the effects of an applied electric field on the morphological change, ion transport and stress build-up in nanoscale thin films. In particular, the relative permittivity of polymers is considered by explicitly introducing dipole characteristics of the polymer CG beads. Detailed study on the kinetics of the response under electric field provides useful insights into the electromechanical response of the thin films. We focused on films containing lamellar forming charged-neutral diblock copolymers, in which interfaces of the microphase separated domains are aligned parallel to the electrodes.

* Corresponding author.
E-mail address: yaof@vt.edu (Y. Fu).

https://doi.org/10.1016/j.cplett.2021.138817
Received 16 December 2020; Received in revised form 9 May 2021; Accepted 7 June 2021
Available online 12 June 2021

The effect of varying dipole moments on the kinetics of the electromechanical responses are studied in detail.

2. Models

2.1. Potentials

The equilibrated ordered lamellar phases of diblock copolymer is obtained by a two-step procedure in the CGMD model as employed in our previous studies [39,40]. Only the key features of this model will thus be described in the following. At first a soft intermolecular potential is used to rapidly equilibrate the diblock copolymers and the ordered lamellar phases can be formed from the initially randomly placed polymers within a comparably short time. The soft intermolecular potential consists of a repulsive interaction similar to those used in dissipative particle dynamics (DPD) simulations [41,42]:

$$U_{ij}^{s} = \begin{cases} \frac{a_{ij}}{2}\left(\frac{r}{r_c}-1\right)^2, r \le r_c \\ 0, r > r_c \end{cases} \quad (1)$$

where a_{ij} represents the interaction strength between monomers of type i and j (i, j = A, B), r_c is the cutoff distance, and r is the distance between two interacting monomers. Here $a_{AA} = a_{BB} = 25.0k_BT$, and $a_{AB} = 50k_BT$. Adjacent beads are connected by a harmonic bond with zero equilibrium length:

$$U_b^s = \kappa_D r^2 \quad (2)$$

where the spring constant $\kappa_D = 1.89k_BT/\sigma^2$. The monomer concentration ρ_N is controlled at a density of 3.0 r_c^{-3}, where r_c is estimated to be 1.65 to keep the similar density between the soft and hard model.

The second step involves a final equilibration with the target potential (hard potential) for a further relaxation of short-range structure. In the target potential all beads interact via a shifted Lennard-Jones (LJ) potential of the form [43,44]

$$U_{ij}^{h} = \begin{cases} 4\epsilon_{ij}\left[\left(\frac{\sigma}{r}\right)^{12} - \left(\frac{\sigma}{r}\right)^{6}\right], r \le 2.5 \\ 0, r > 2.5 \end{cases} \quad (3)$$

where ϵ_{ij} is the interaction strength in the hard potential between beads of type i and j (i, j = A, B), and σ is the diameter of bead. $\epsilon_{AA} = \epsilon_{BB} = 1.0k_BT$, and $\epsilon_{AB} = 0.1k_BT$. In addition, adjacent beads interact via a harmonic potential

$$U_b^h = \kappa(r-\sigma)^2 \quad (4)$$

with bond constant $\kappa = 200k_BT/\sigma 2$, and k_B and T represent the Boltzmann constant and temperature, respectively. Other modeling details of the two-step equilibrium can also be found in our previous studies [39,40].

The relative permittivity (or dielectric constant) ϵ_r of the diblock copolymers are considered by introducing freely rotating permanent dipole moment μ to all neutral beads. The dipole moment μ varies from 1 to 2 to represent moderately to strongly polar polymers. The mapping from the reduced dipole moment to that of the realistic material system can be conducted through $\mu = \mu^*/\sqrt{4\pi\varepsilon_0\sigma^3\epsilon}$, where μ^* is the dipole moment in physical unit. Using $\sigma \sim nm$ and $\epsilon = 1k_BT$, it can be estimated that the reduced dipole of materials having the dielectric constant of 10 is around 1, and that a reduced dipole of 1–2 corresponds to the ϵ_r in the range of 10∼50. This falls into the range for moderately to strongly polar polymeric materials. The estimated value would vary depending on the specific value of repeat unit size σ and interaction strength ϵ.

The electrostatic interaction among the negatively charged beads, positively charged counterions and neutral beads containing permanent dipoles are turned on in the target potential:

$$U_{coul/dipole}^{h} = \begin{cases} \frac{q^2}{r} + \frac{q}{r^3}\left(\vec{p}_j \cdot \vec{r}\right) + \frac{1}{r^3}\left(\vec{p}_i \cdot \vec{p}_j\right) - \frac{3}{r^5}\left(\vec{p}_i \cdot \vec{r}\right)\left(\vec{p}_j \cdot \vec{r}\right), r < 12\sigma \\ 0, r \ge 12\sigma \end{cases} \quad (5)$$

where q is the charge of the positively charged beads and negatively charged counterions, $\vec{p}$ is the vector of the dipole moment and $\vec{r} = R_i - R_j$ is relative position vector between atom i and j.

The above model will be referred as 'dipole model'. A uniform background dielectric without explicit dipole description, one of the most commonly used models, will also be studied in order to make comparison with the dipole model.

2.2. Simulation procedure

The block copolymers under consideration has a chain length N of 100, and the fraction of A block f_A equals to 0.5. A total of 200 chains are simulated. For ionic copolymers, 30% of the type A bead are charged, and charged beads are distributed uniformly along the A block. To keep the system charge neutral, 3,000 counterions are also introduced. The polymer and counterion beads are randomly displaced in the simulation box with an initial density of around 0.85 σ^{-3}.

Before investigating the thin film, the bulk copolymers are first studied, where periodic boundary condition is applied to all directions. An NPT ensemble is adopted, with constant pressure set as zero and thermostat coupling constant equal to 0.5 τ^{-1}. A comparison between the ion transport behaviors predicted by the model that adopts the dipole description for each bead and that uses a uniform background dielectric constant is conducted. The other potentials involved in describing the two models remain the same.

In the case of thin films, an NVT ensemble is adopted with shrink-wrapped boundary condition applied in the z direction while the other two directions kept periodic. The thickness of the film is adjusted so that the pressure along all directions fluctuate around zero. Polymer beads and counterions also experience interaction from the walls that are located at the shrink-wrapped boundary representing either the substrate or electrode. At the soft potential stage, the B type monomer is experiencing more repulsion than the other atoms from the wall, when the interaction strength between the wall and B type is $a_{W-B} = 50k_BT$ and that between the wall and A type is $a_{W-A} = 25.0k_BT$ so that the neutral layer is formed in the middle of the film. In the target potential stage, the nonbonded LJ potential parameter is set as $\epsilon = 1k_BT$ between the wall and polymer beads, as well as between counterions and other beads.

For both the bulk and thin film systems, the soft potential stage takes for 0.5∼2 million timesteps at a time step size of 0.01 τ until the lamellar phase is generally formed. Then a further equilibration for the short-range structure is conducted for another 2∼6 million steps at a time-

step size of 0.005 τ. All simulations were performed using the LAMMPS Molecular Dynamics Simulator at a constant temperature of $1\epsilon/k_B$. The electric field strength $E = 5$ corresponds to hundreds of V/μm based on $E = E^*\sqrt{4\pi\varepsilon_0\sigma^3/\epsilon}$ using σ *nm* and $\epsilon = 1k_BT$, where E^* is the electrical field in physical unit and k_B is the Boltzmann constant. This is a quite strong electric field mainly because it takes prohibitively long computational time to reach a steady state under weaker electric field using a MD simulation.

In the following, the standard reduced LJ units are used, i.e., all physical quantities are expressed in the units of m, σ, ε, and k_B unless otherwise specified.

3. Result

3.1. Mean squared displacement (MSD) of ionic copolymers in bulk condition

The ionic copolymers with 30% A block charged are first investigated in bulk condition. The time dependent mean squared displacement (MSD) curves are plotted in the logarithmic plot. In the model that includes explicit dipole description, the diffusion of counterions is slower compared to that using the uniform background dielectric model, regardless of the magnitude of dipole moment (Fig. 1a). In the long-time regime ($t > 100$), the counterions in both models show diffusive behavior.

The MSD of the neutral monomers, charged monomers and counterions are shown in Fig. 1b and c. In the uniform dielectric model, the

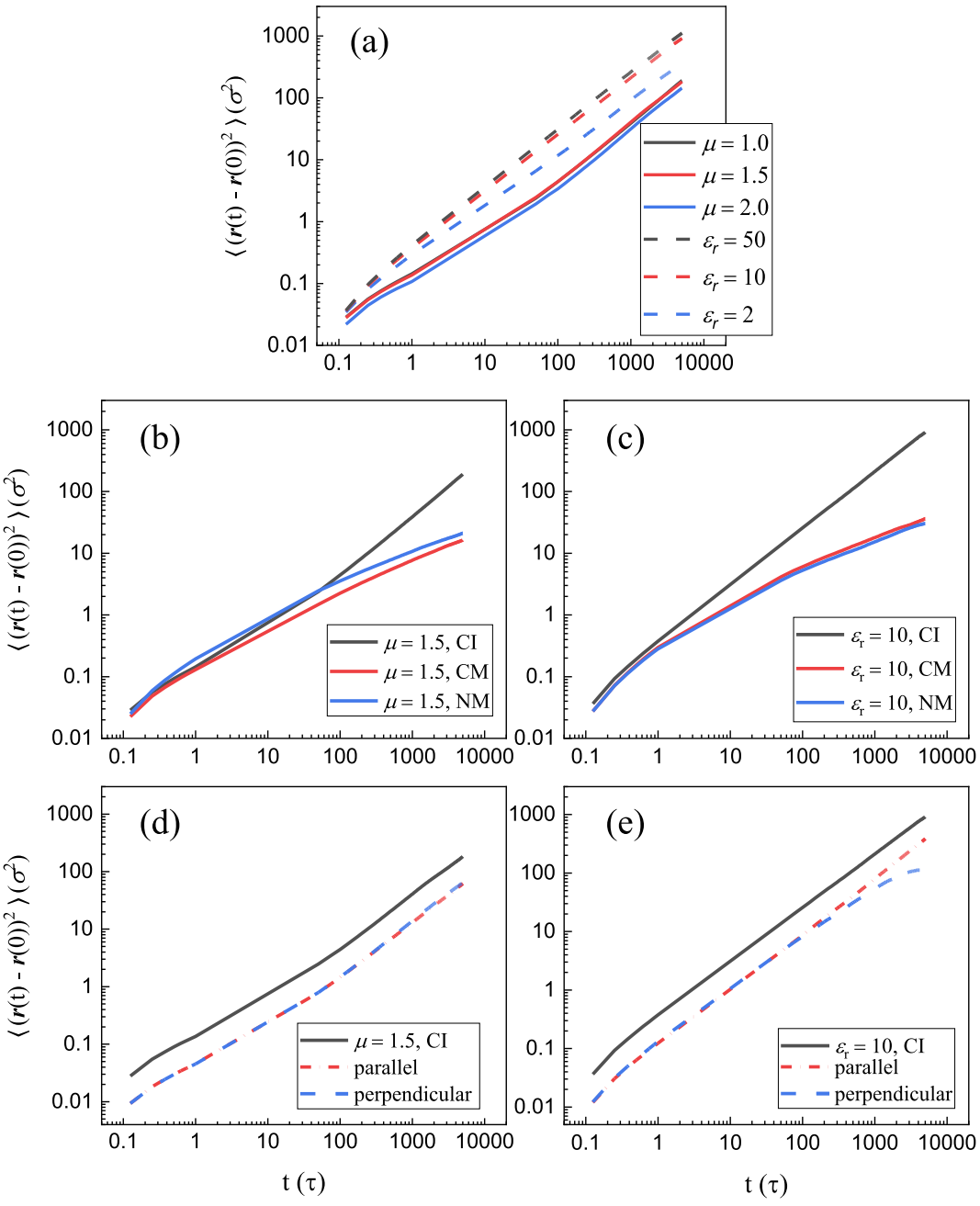

Fig. 1. (a) MSD of the counterion in two models; (b) and (c) MSD of atom groups of counterion (CI), charged monomers (CM) and neutral monomers (NM) in dipole and KG model, respectively; (d) and (e) the MSD of counterion and its component in direction perpendicular and parallel to the lamellae of dipole and KG model.

neutral monomers show a transition from ballistic regime to $t^{1/2}$ and then to $t^{1/4}$, as predicted by the sub-diffusion motion of unrestricted Rouse model and Rouse motion confined to a tube, respectively. The neutral monomers in the dipole model demonstrate different transition behaviors that occur at the larger time scale and higher diffusivity. The charged monomers show lower diffusivity than neutral ones in the dipole model, due to their stronger interaction with the neutral beads with dipole. In both models, the counterions start to decouple from the monomer movement in the long-time scale. However, the decoupling effect is more pronounced in the uniform dielectric model.

In Fig. 1d and e, the MSD of counterions is decomposed into the parallel and perpendicular to the interface normal direction. In the uniform dielectric model, the diffusion of the perpendicular component of counterion MSD is significantly different from the parallel component after $t > 1,000$, when the mobility of counterion drops in the perpendicular direction. In this model, the counterion only interact strongly electrostatically with the charged monomers and preferably reside in the A block. Since the block thickness is around 10, the reduced perpendicular mobility at this length scale should be related to the constrained movement of counterions within the A block. In the dipole model, the counterions interact electrostatically with both the charged and neutral monomers, so that the mobilities in the two directions are comparable.

The extracted diffusion coefficients of the counterions and monomers (both charged and neutral) in the lamellar BCPs for both the dipole and uniform dielectric models with different dipole moment μ and dielectric constant ε_r are given in Table 1. The diffusion coefficient of monomer D_{mo} and counterion D_{ci} decreases with increasing μ due to the stronger interaction between monomers and counterions. Due to the weak interaction between counterion and neutral monomers, D_{ci} is much higher in the uniform dielectric model. The perpendicular and parallel diffusion coefficients are very similar for the dipole model as analyzed above. It can be seen that even though a uniform background dielectric constant can be more conveniently employed in the MD model to represent the polar polymers, it predicts different ion diffusion behaviors from the explicit dipole model. In the following, the ion transport, stress and morphology evolution are investigated in the thin film structure described by the dipole model.

3.2. The response of neutral copolymer thin film to external electric field

The neutral BCPs with and without dielectric mismatch (i.e., the A and B block are assigned with the same or different dipole moment) is then considered before the ionic BCP thin film. The stable morphology and that after the applied electric field of neutral monomers with and without dielectric mismatch are shown in Fig. 2. The neutral BCP with dielectric mismatch shows a much sharper interface comparing to the BCP without mismatch, indicating that the immiscibility of the two blocks becomes stronger with increasing dielectric mismatch. From a microscopic point of view, the A and B type bead at $\mu_A = 0$and $\mu_B = 2.0$ will not attract each other electrostatically, reducing the possibility of miscibility.

Under an applied electric field, the mismatched BCPs demonstrate a transition with the lamellae microphase interface realigning to the parallel to electric field direction. This phenomenon has been discussed in several experimental and theoretical papers [6,7]. In contrast, the neutral BCPs with no dielectric mismatch remain their morphology upon the applied electric field. The consistent results between our model and previous studies on neutral polymers support the validity of the dipole model.

Table 1
Diffusion coefficient of neutral monomers (D_{mo}) and counterions (D_{ci}) extracted from the MSD plot in the long-time scale; subscript $\perp$ and $\|$ indicate perpendicular and parallel to the interface normal direction, respectively.

	$\mu = 1.0$	$\mu = 1.5$	$\mu = 2.0$	$\varepsilon_r = 10$	$\varepsilon_r = 50$
D_{mo}	6.27E-05	4.97E-05	4.26E-05	5.34E-05	4.76E-05
D_{ci}	1.12E-03	1.09E-03	7.90E-04	4.63E-03	5.66E-03
$D_{ci\perp}$	3.38E-04	3.51E-04	2.52E-04	1.63E-04	9.25E-05
$D_{ci\|}$	3.93E-04	3.71E-04	2.69E-04	2.40E-03	3.00E-03

3.3. The response of ionic copolymers thin film to external electric field

3.3.1. Ion dissociation

The number of neighboring counterions of the charged monomers is analyzed to reveal the dissociation of charged pairs under the electric field. The average number of counterions $\langle n \rangle$ is calculated based on a cutoff distance of 2.5 and averaged over all charged monomers. As shown in Fig. 3, $\langle n \rangle$ is around 3.4 for all cases before the electric field is applied. After the electric field is applied, dissociation occurs as shown by the decreasing $\langle n \rangle$ within $t = 700, 3,500$and $5,000$ for different $\mu = 1, 1.5$ and 2, respectively. This happens simultaneously with the rapid decrease of $\mu_{t,z}$. Then $\langle n \rangle$ gradually reaches a stable value. This dissociation process is accompanied with the transport of charged monomers and counterions, and the evolution of morphology. The decrease in moment magnitude is more pronounced with increasing dipole moment.

The time-dependent evolution of total dipole moment component $\mu_{t,x}$, $\mu_{t,y}$ and $\mu_{t,z}$ is calculated to understand the effect of external electric field as shown in Fig. 4. Under no external electric field, the value of $\mu_{t,x}$, $\mu_{t,y}$ and $\mu_{t,z}$ are fluctuating around zero, indicating that the dipole moments of neutral monomers are randomly oriented reaching electrostatic balance. The $\mu_{t,z}$ of the system with $\mu = 1.0, 1.5$ and 2.0 induced by electric field reaches around 8,700, 14,000 and 18,000 at the peak, respectively. The total dipole moment perpendicular to the electric field $\mu_{t,x}$ and $\mu_{t,y}$ continues to fluctuate around zero. With the system further evolving under the electric field, $\mu_{t,z}$ decreases and gradually stabilized. The time to reach a stabilized value increases with increasing μ. At the plateau, the $\mu_{t,z}$ fluctuates around zero except for the system with $\mu = 2.0$ which still slowly decreases. At this stage, the BCP enters a stable or a quasi-stable state under the electric field, which will be further discussed in the following sections.

3.3.2. Stress evolution

The stress evolution contributed from the monomers and counterions at varying dipole moment μ are plotted in Fig. 5. The normal stress component σ_{zz} and $\frac{1}{2}(\sigma_{xx}+\sigma_{yy})$ are used to describe the stress parallel and perpendicular to the electric field. The stress evolution of the systems with different dipole moment is quite different, but all can be roughly divided into three stages marked by the dashed line.

For $\mu = 1.0$, both counterions and monomers have a rapid decrease in $\frac{1}{2}(\sigma_{xx}+\sigma_{yy})$at $t < 700$ (stage I), showing a strong compression perpendicular to the electric field. σ_{zz} also decreases at this stage. As will be shown later, counterions and charged monomers are moving toward the corresponding electrode at this stage. At stage II ($700 < t < 3,300$), σ_{zz} is relatively stable and $\frac{1}{2}(\sigma_{xx}+\sigma_{yy})$ decreases at a relatively slow rate. The time evolution of stress at these stages can also be related to the change of $\mu_{t,z}$ in Fig. 4.

With increasing dipole moment, the effect of electric field on the stress from monomers and counterions contribution is more complex in systems with $\mu = 1.5$ and $\mu = 2.0$. At stage I, the curve following the same pattern as the stage I at $\mu = 1.0$, which is also dominated by the movement of charged monomers and counterions (Fig. 5), as also indicated by the dissociation of charged pairs during this time period (Fig. 3). At stage II, $\frac{1}{2}(\sigma_{xx}+\sigma_{yy})$ increases and σ_{zz} continues to decrease (Fig. 5). At stage III, the plateau is formed for all stress components. At this stage, the film can be considered to have reached a steady state (Fig. 5).

The morphology, density and stress distribution along the film thickness are further examined in the following. As shown in Fig. 6, for

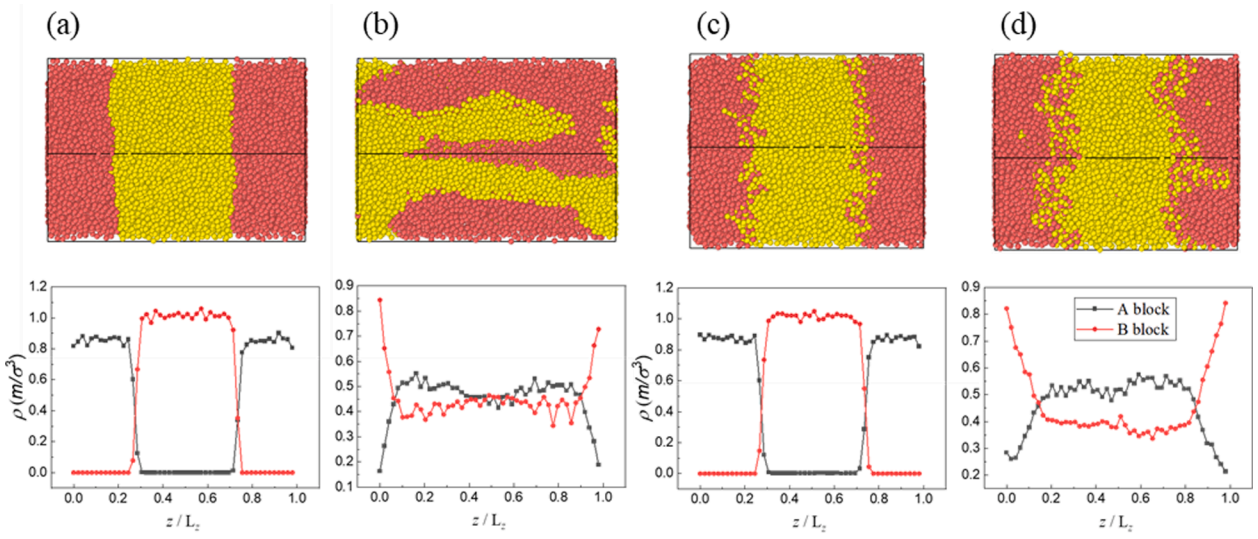

Fig. 2. Steady state of neutral BCP thin film with dielectric mismatch ($\mu_A = 0, \mu_B = 2.0$)at (a) $E = 0$ and (b) $E = 5$. Steady state of neutral BCP with ($\mu_A = \mu_B = 2.0$)at (a) $E = 0$ and (b) $E = 5$. A block is in red and B block is in yellow.

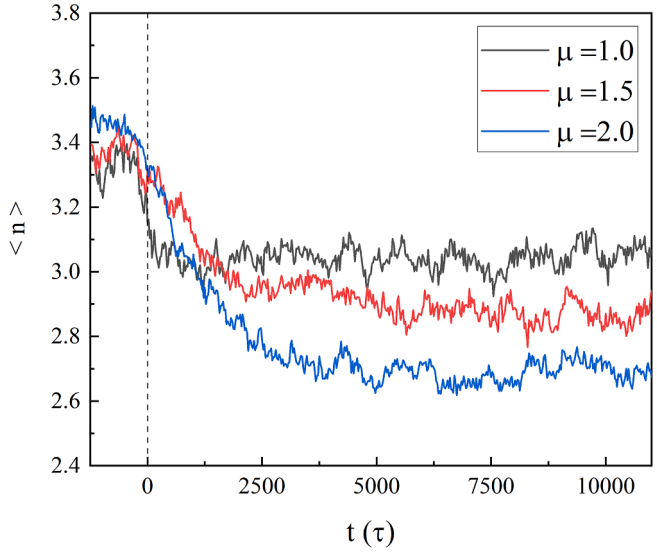

Fig. 3. Computed averaged neighboring counterions number $\langle n \rangle$ of charged monomers over time; the dashed line represents that the electric field is turned on at $t = 0$.

$\mu = 1.0$ the counterions are mainly scattered in the A block at the initial stage. There are a small number of counterions in the B block causing larger stress fluctuation due to the lack of positively charged monomers in the neighbors (Fig. 6 upper panel c). After the electric field is applied, counterions and charged monomers are found to migrate to and accumulate on the surface of the positive and negative walls, respectively. This can be clearly seen in the density profile of the A block polymers and counterions. The stress of counterions changes significantly, showing a linear profile across the film thickness. In comparison, the stress of monomers only shows relatively small perturbation by the applied electric field at the locations close to the walls.

The morphology, density and stress distribution along the thin film thickness at $\mu = 1.5$ can be more clearly seen in Fig. 7. At the initial state when $E = 0$, a higher number of counterions are found in the B block as compared to $\mu = 1.0$, possibly due to the stronger interaction between the counterions and monomers of higher dipole moment. The morphology and density profile at the end of stage I shows that the counterions have already largely migrated to the negative wall at $t = 3,000$. A few A-block copolymers initially layered at the negative wall migrate towards the positive wall, forming several bridges between the two A-block layers, similar to that observed for $\mu = 1.0$. The migration of A-block through bridges continues and finishes at the end of stage II around $t = 12,000$. At stage III, the BCP thin film reaches a new stable state under the applied electric field, where the B block location is shifted toward the negative wall compared to the initial state.

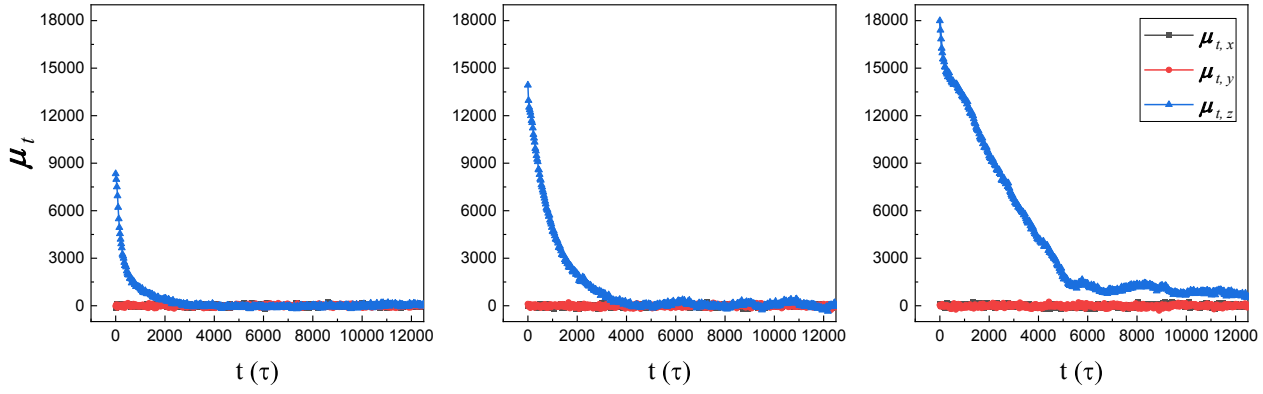

Fig. 4. Evolution of the total dipole moment component with time after the electric field is applied. The left, middle, and right panel corresponds to $\mu = 1.0, 1.5$ and 2.0 respectively.

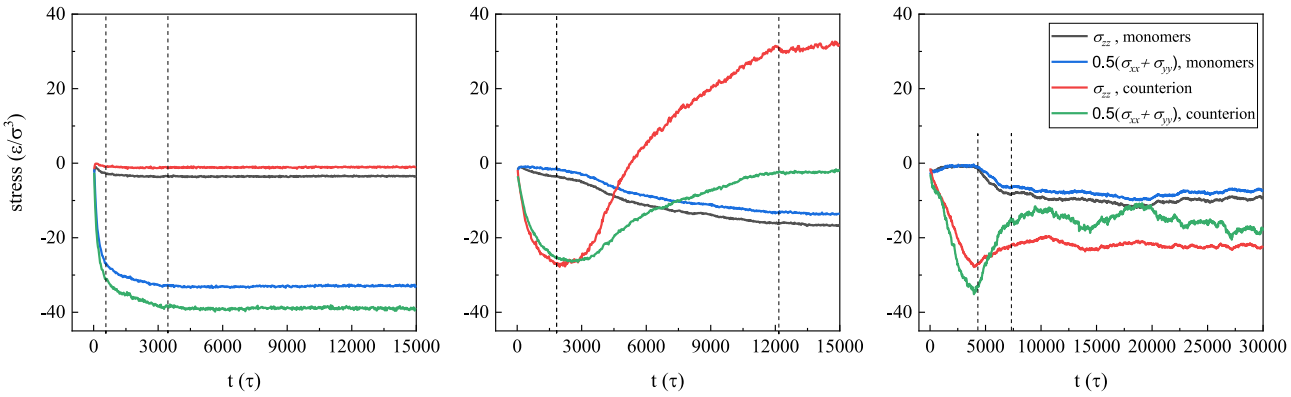

Fig. 5. Evolution of the stress component contributed from the monomers and counterions with time when electric field is applied at $t = 0$. The left, middle, and right panel corresponds to $\mu = 1.0, 1.5$ and 2.0 respectively.

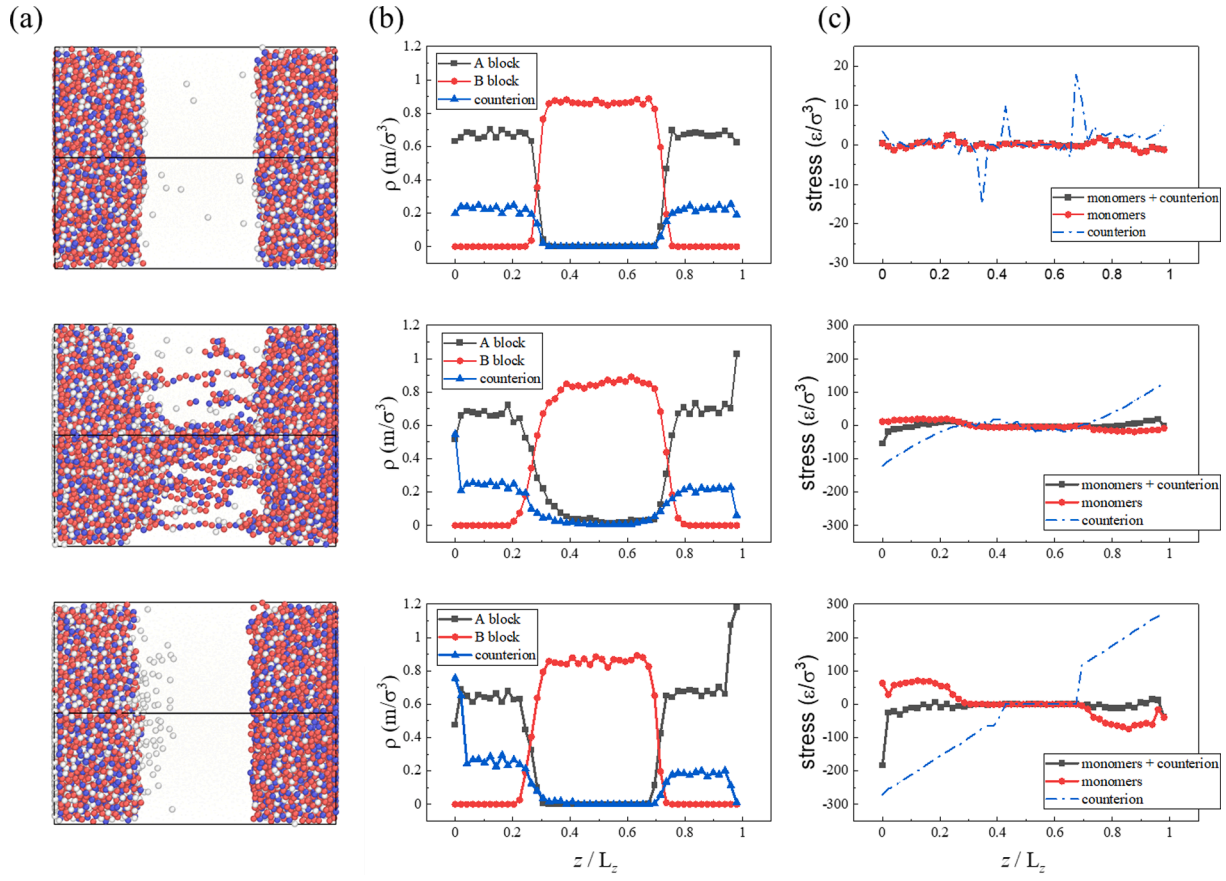

Fig. 6. (a) Morphology, (b) density distribution and (c) stress distribution along the height of the film thickness at different stages of BCPs with $\mu = 1.0$. The upper, middle and lower panel represents the initial stage, stage I and III at $t = 0$,500, and 12, 000, respectively. The B type monomer are set as transparent for better visualization; counterion, charged monomer and neutral A type monomer are in white, red and blue respectively.

At $\mu = 2.0$, the interface roughness increases greatly with a number of protrusions of A blocks into the B block, which increases the stress near the interface due to the low compatibility between the A and B block (Fig. 8 upper panel a). The density profile shows the transition between blocks becomes smoother. After the applied electric field, the lamellar morphology transforms into a disordered phase within very short time ($\sim$500 τ). This disordered phase is maintained until stage II. Eventually the morphology become stable as shown in Fig. 8a bottom panel. Even though a separated microphase morphology is expected as for $\mu = 1.0$ and 1.5, this microstructure maintains the same up to a simulation time of $t = 25,000$.

Overall, the surface roughness at the initial state is greatly affected by the dipole moment μ. With increasing μ, the lamellar interfacial width becomes larger. The response of thin film under the applied electric field is also affected by the dipole moment, with a well-separated microphase under electric field at $\mu = 1.0$ and 1.5, and a mixed phase at $\mu = 2.0$. Under all conditions, the counterions and A block with charged monomers migrate to the corresponding positive and negative wall, respectively, and the density of the accumulated counterions and charged monomers are around 0.75 and 1.15, respectively. The A block migration is through bridges formed in the B block at stage I. At the final stage, the A block initially located at the positive wall is either reduced in

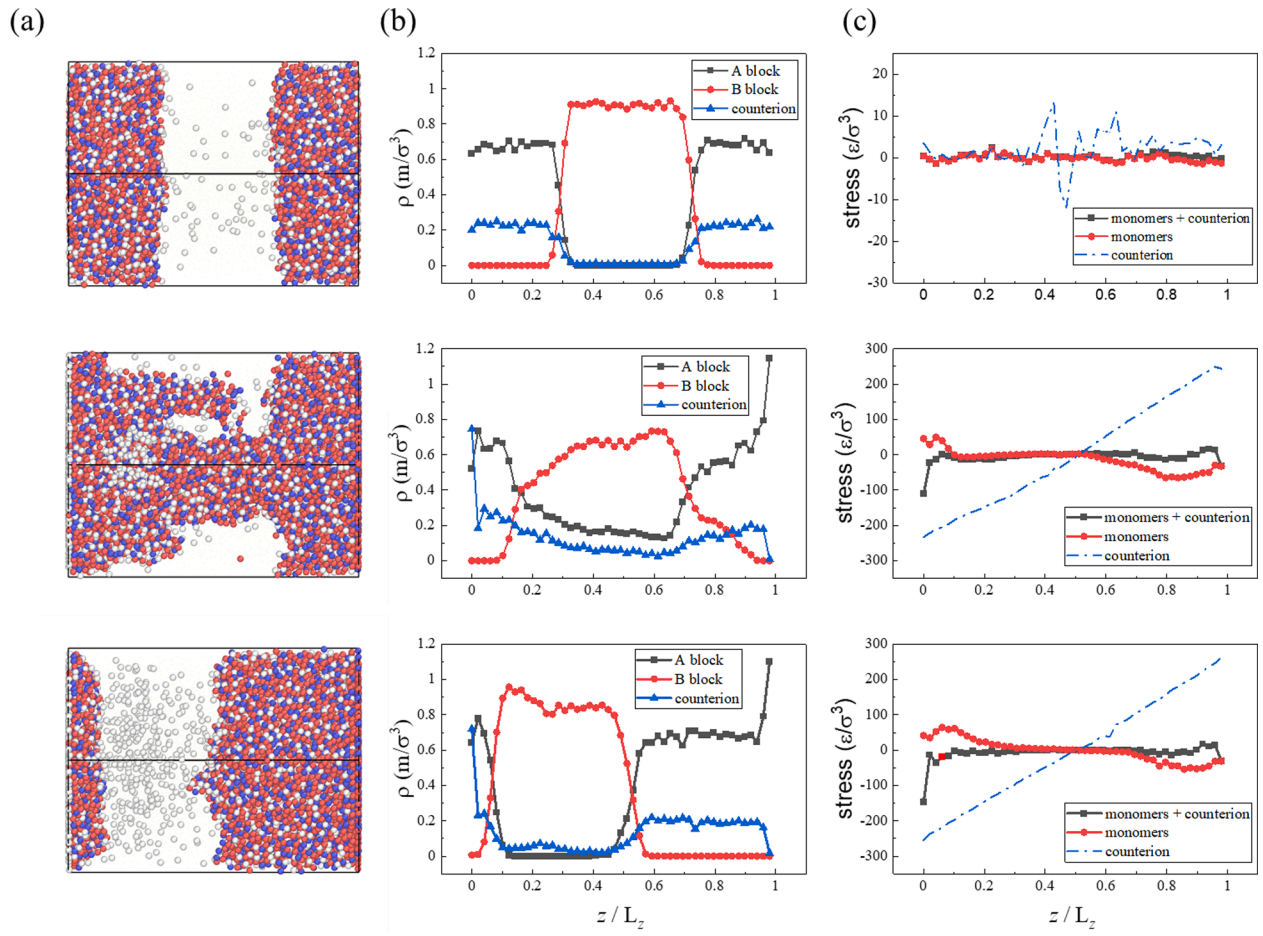

Fig. 7. (a) Morphology, (b) density distribution and (c) stress distribution along the height of the film thickness at different stages of BCPs with $\mu = 1.5$. The upper, middle and lower panel represents the initial stage, stage I and III at $t = 0,3,000,15,000$, respectively. The B type monomer are set as transparent for better visualization; counterion, charged monomer and neutral A type monomer are in white, red, and blue respectively.

thickness or eliminated, and the B blocks are shifted to the positive wall.

At last, the model is modified by introducing dipole to the charged beads in order to consider the case of large organic unit. The BCPs with $\mu = 1.5$ is modified with all monomers assigned with dipole moment regardless of their charge state. As shown in Fig. 9, the initial interface sharpness appears similar as the case when the charged monomer has no dipole moment presented above. However, the extra dipole moment could potentially increase the attraction between beads, and reduce their mobility. It is observed that it takes longer time for the system to reach a steady state with this modification. The morphology at $t = 15{,}000\ \tau$ still shows a transient state and the stress still evolves.

So far, there have been limited experimental studies on the response of ionic polymers to strong electric field. Existent experimental and theoretical studies have been relatively focused on the neutral BCPs, which demonstrate drastic changes in morphology by the reorientation of the lamellar phases with microdomain interfaces parallel to the electric field [38,45]. This reorientation is mainly related to the dielectric mismatch between the two blocks, which has also been captured in our model. Electric-field induced motion of ionic copolymer thin films has only been studied by Dugger et al. [46], where the change in the thickness of lamellar thin film and couterion redistribution has been reported. These studies are in qualitative agreement with our findings, even though quantitative comparison is difficult due to the difference in the field strength and the employment of a CG model in our study. In addition, theoretical and experimental studies have revealed the influence of physical properties of constituent copolymers including the dielectric contrast on the interfacial width and roughness of BCP film [47]. This is also captured in our studies in that block copolymer with $\mu = 1.0$ and 1.5 show a relatively sharp interface. With increase polarizability, a wider and rougher interfacial area is found for $\mu = 2.0$ indicating the compatibility of the two blocks is increased.

4. Conclusion

In this study, CGMD simulations are performed to understand the response of the ionic diblock copolymer thin film under electric field. The dipole model is adopted to describe the neutral monomers. The mobility of counterions and monomers are first compared with the uniform dielectric model. The MSD analysis shows that the diffusion behaviors described are similar but exhibit differences in the diffusion coefficients and diffusivity parallel and perpendicular to the interface normal direction. Compared with the uniform dielectric model, the counterions in the dipole model are less confined within the A block.

The response of the BCP thin film under the strong electric field is carefully analyzed in terms of the ion transport, morphology and stress evolution. Different dipole moment that represents different relative permittivity is considered. The evolution has been largely divided into three stages as follows:

I. Stage I: Counterions and charged monomers move towards the negative and positive wall, accompanied by the dissociation between charge monomers and counterions. The total dipole moment in the electric field direction also relaxes from the rapid initial increase caused by the electric field. At $\mu = 1.0$ and 1.5, the transport of charged monomers is mainly through a few bridges connecting A blocks rapidly formed under the applied electric

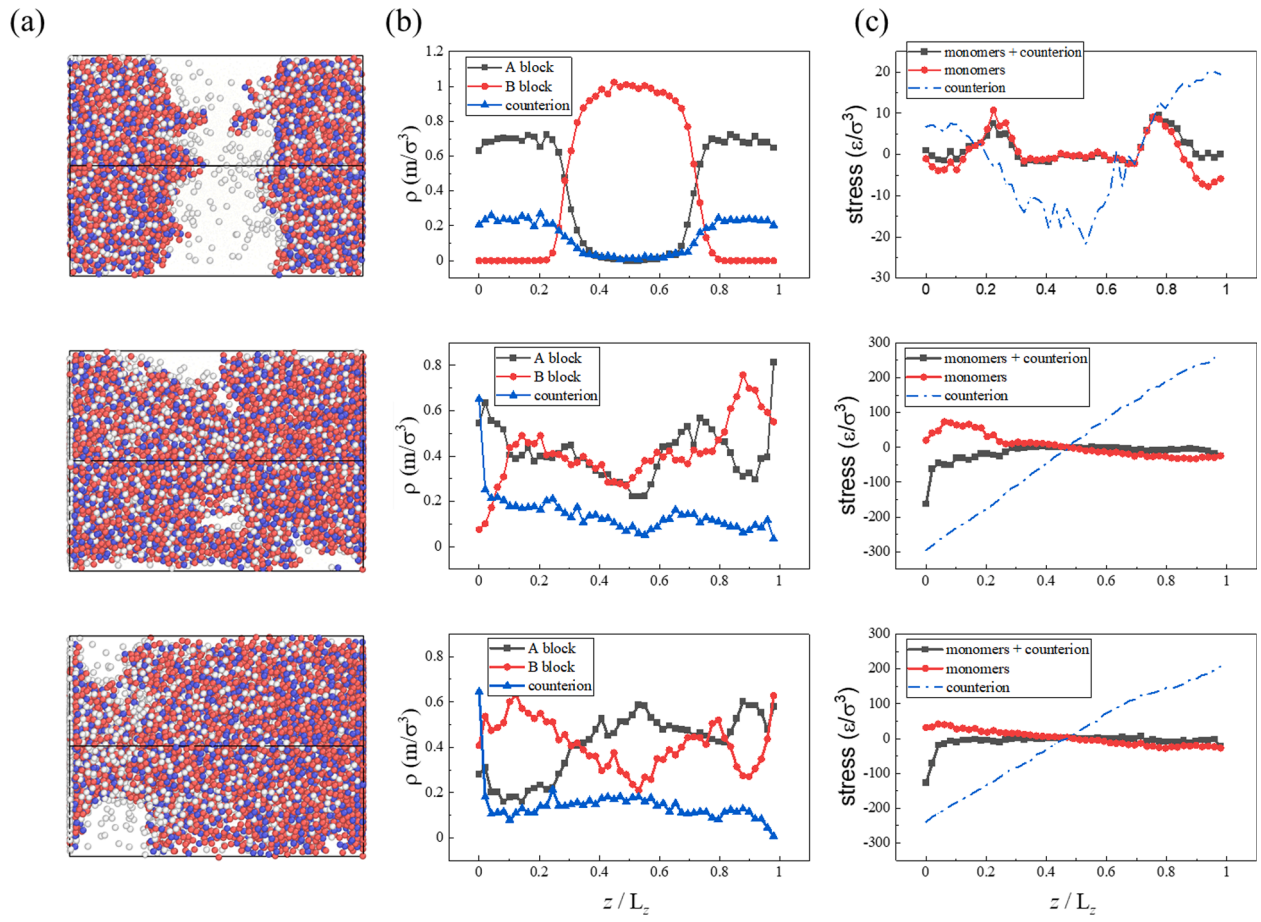

Fig. 8. (a) Morphology, (b) density distribution and (c) stress distribution along the height of the film thickness at different stages of BCPs with $\mu = 2.0$. The upper, middle and lower panel represents the initial stage, stage III and III at $t = 0, 4,500, 15,000$, respectively. The B type monomer are set as transparent for better visualization; counterion, charged monomer and neutral A type monomer are in white, red and blue respectively.

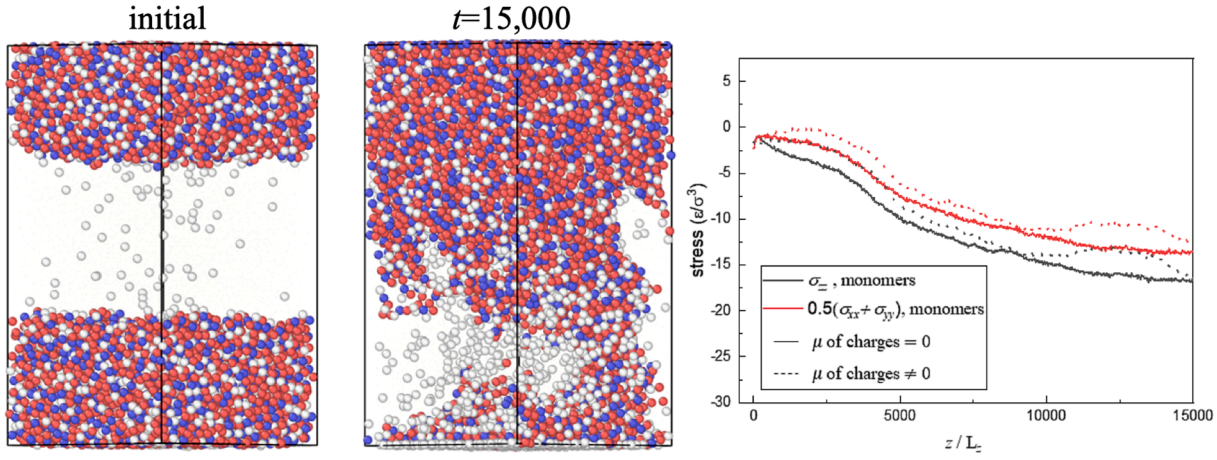

Fig. 9. The morphology of modified model at $\mu = 1.5$ before the electric field is applied and that 15,000 τ after the electric field is applied, as well as the evolution of stress over time, where solid and dashed lines represent the model with charged monomer without and with a dipole moment, respectively.

field. At $\mu = 2.0$, the well-separated microphase becomes disordered at this stage.

II. Stage II: At relatively low dielectric constant (i.e., $\mu = 1.0$ and 1.5), the thickness and number of bridges reduces. At $\mu = 2.0$, the B block polymer starts to gather near the positive wall. Meanwhile, A type monomers gradually move out of that region. The dissociation of charged pairs has been largely completed, and the dipole moment undergo further reorientation, accompanied with stress relaxation. Even though the polymer transport continues, the dissociation of charged pairs has stopped, and the total moment $\mu_{t,z}$ remains a plateau.

III. Stage III: The BCP thin film reaches a steady state. At $\mu = 1.0$ and 1.5, A block bridges disappear leaving a well-separated lamellae morphology. At $\mu = 2.0$, B block is partially gathered close to the wall and partially mixed with A block.

This CG model with explicitly introduced dipole moment to represent electric permittivity is able to capture some salient features consistent with experimental and theoretical studies such as the morphology change, counterion redistribution, and interface roughness under applied electric field.

CRediT authorship contribution statement

Mengze Ma: Conceptualization, Methodology, Validation, Formal analysis, Investigation, Data curation, Writing - original draft, Writing - review & editing, Visualization. **Yao Fu:** Conceptualization, Methodology, Validation, Formal analysis, Resources, Data curation, Writing - original draft, Writing - review & editing, Visualization, Supervision, Project administration, Funding acquisition.

Declaration of Competing Interest

The authors declare that they have no known competing financial interests or personal relationships that could have appeared to influence the work reported in this paper.

Acknowledgements

This research was supported by the National Institute for Occupational Safety and Health through the Pilot Research Project Training Program of the University of Cincinnati Education and Research Center Grant #T42OH008432.

References

[1] Y. Tsori, D. Andelman, C.-Y. Lin, M. Schick, Block Copolymers in Electric Fields: A Comparison of Single-Mode and Self-Consistent-Field Approximations, Macromolecules 39 (2006) 289–293.
[2] Y. Tsori, D. Andelman, Coarse graining in block copolymer films, J. Polym. Sci., Part B: Polym. Phys. 44 (2006) 2725–2739.
[3] D. Andelman, R.E. Rosensweig, Modulated Phases: Review and Recent Results, J. Phys. Chem. B 113 (2009) 3785–3798.
[4] C.-Y. Lin, M. Schick, D. Andelman, Structural Changes of Diblock Copolymer Melts Due to an External Electric Field: A Self-Consistent-Field Theory Study, Macromolecules 38 (2005) 5766–5773.
[5] Y. Tsori, D. Andelman, Thin Film Diblock Copolymers in Electric Field: Transition from Perpendicular to Parallel Lamellae, Macromolecules 35 (2002) 5161–5170.
[6] M.W. Matsen, Converting the nanodomains of a diblock-copolymer thin film from spheres to cylinders with an external electric field, J. Chem. Phys. 124 (2006), 074906.
[7] M.W. Matsen, Stability of a Block-Copolymer Lamella in a Strong Electric Field, Phys. Rev. Lett. 95 (2005), 258302.
[8] W. Gu, H. Zhao, Q. Wei, E.B. Coughlin, P. Theato, et al., Line Patterns from Cylinder-Forming Photocleavable Block Copolymers, Adv. Mater. 25 (2013) 4690–4695.
[9] S. Gupta, Q. Zhang, T. Emrick, T.P. Russell, "Self-Corralling" Nanorods under an Applied Electric Field, Nano Lett. 6 (2006) 2066–2069.
[10] S. Mogurampelly, V. Ganesan, Effect of Nanoparticles on Ion Transport in Polymer Electrolytes, Macromolecules 48 (2015) 2773–2786.
[11] T. Irita, D. Chen, X. Li, J. Wang, T.P. Russell, Thin Films of Semifluorinated Block Copolymers Prepared by ATRP, Macromol. Chem. Phys. 212 (2011) 2399–2405.
[12] C.-Y. Lin, M. Schick, Self-consistent field study of the alignment by an electric field of a cylindrical phase of block copolymer, J. Chem. Phys. 125 (2006), 034902.
[13] K. Schmidt, C.W. Pester, H.G. Schoberth, H. Zettl, K.A. Schindler, et al., Electric Field Induced Gyroid-to-Cylinder Transitions in Concentrated Diblock Copolymer Solutions, Macromolecules 43 (2010) 4268–4274.
[14] M. Ruppel, C.W. Pester, K.M. Langner, G.J.A. Sevink, H.G. Schoberth et al., Electric Field Induced Selective Disordering in Lamellar Block Copolymers, 7 (2013) 3854-3867.
[15] C.W. Pester, K. Schmidt, M. Ruppel, H.G. Schoberth, A. Böker, Electric-Field-Induced Order-Order Transition from Hexagonally Perforated Lamellae to Lamellae, Macromolecules 48 (2015) 6206–6213.
[16] K. Schmidt, H.G. Schoberth, M. Ruppel, H. Zettl, H. Hänsel, et al., Reversible tuning of a block-copolymer nanostructure via electric fields, Nat. Mater. 7 (2008) 142–145.
[17] H.G. Schoberth, K. Schmidt, K.A. Schindler, A. BöKer, Shifting the order−disorder transition temperature of block copolymer systems with electric fields, Macromolecules 42 (2009) 3433–3436.
[18] T. Tanaka, I. Nishio, S.T. Sun, S. Ueno-Nishio, Collapse of Gels in an Electric Field, Science 218 (1982) 467–469.
[19] D.F. Miranda, C. Versek, M.T. Tuominen, T.P. Russell, J.J. Watkins, Cross-Linked Block Copolymer/Ionic Liquid Self-Assembled Blends for Polymer Gel Electrolytes with High Ionic Conductivity and Mechanical Strength, Macromolecules 46 (2013) 9313–9323.
[20] O. Kim, S.Y. Kim, B. Park, W. Hwang, M.J. Park, Factors Affecting Electromechanical Properties of Ionic Polymer Actuators Based on Ionic Liquid-Containing Sulfonated Block Copolymers, Macromolecules 47 (2014) 4357–4368.
[21] M. Shahinpoor, Y. Bar-Cohen, J.O. Simpson, J. Smith, Ionic polymer-metal composites (IPMCs) as biomimetic sensors, actuators and artificial muscles - a review, Smart Mater. Struct. 7 (1998) R15.
[22] Y. Bahramzadeh, M. Shahinpoor, A Review of Ionic Polymeric Soft Actuators and Sensors, Soft Rob. 1 (2013) 38–52.
[23] J.-H. Choi, Y. Ye, Y.A. Elabd, K.I. Winey, Network Structure and Strong Microphase Separation for High Ion Conductivity in Polymerized Ionic Liquid Block Copolymers, Macromolecules 46 (2013) 5290–5300.
[24] R. Kumar, V. Bocharova, E. Strelcov, A. Tselev, I.I. Kravchenko et al., Ion transport and softening in a polymerized ionic liquid. 7 (2015) 947-955.
[25] V. Bocharova, A.L. Agapov, A. Tselev, L. Collins, R. Kumar, et al., Controlled Nanopatterning of a Polymerized Ionic Liquid in a Strong Electric Field, Adv. Funct. Mater. 25 (2015) 805–811.
[26] G.G. Putzel, D. Andelman, Y. Tsori, M. Schick, Ionic effects on the electric field needed to orient dielectric lamellae, J. Chem. Phys. 132 (2010), 164903.
[27] A. Dehghan, M. Schick, A.-C. Shi, Effect of mobile ions on the electric field needed to orient charged diblock copolymer thin films, J. Chem. Phys. 143 (2015), 134902.
[28] P. Knychała, M. Banaszak, N.P. Balsara, Effect of Composition on the Phase Behavior of Ion-Containing Block Copolymers Studied by a Minimal Lattice Model, Macromolecules 47 (2014) 2529–2535.
[29] J.-Y. Wang, W. Chen, J.D. Sievert, T.P. Russell, Lamellae Orientation in Block Copolymer Films with Ionic Complexes, Langmuir 24 (2008) 3545–3550.
[30] M.T. Irwin, R.J. Hickey, S. Xie, F.S. Bates, T.P. Lodge, Lithium Salt-Induced Microstructure and Ordering in Diblock Copolymer/Homopolymer Blends, Macromolecules 49 (2016) 4839–4849.
[31] A.S. Bodrova, E.Y. Kramarenko, I.I. Potemkin, Microphase Separation Induced by Complexation of Ionic−Non-Ionic Diblock Copolymers with Oppositely Charged Linear Chains, Macromolecules 43 (2010) 2622–2629.
[32] M. Goswami, R. Kumar, B.G. Sumpter, J. Mays, Breakdown of Inverse Morphologies in Charged Diblock Copolymers, J. Phys. Chem. B 115 (2011) 3330–3338.
[33] R. Kumar, B.G. Sumpter, S.M. Kilbey, Charge regulation and local dielectric function in planar polyelectrolyte brushes, J. Chem. Phys. 136 (2012), 234901.
[34] C.E. Sing, J.W. Zwanikken, M. Olvera de la Cruz, Electrostatic control of block copolymer morphology, Nat. Mater. 13 (2014) 694–698.
[35] D. Ben-Yaakov, D. Andelman, D. Harries, R. Podgornik, Beyond standard Poisson-Boltzmann theory: ion-specific interactions in aqueous solutions, J. Phys.: Condens. Matter 21 (2009), 424106.
[36] G. Ariel, D. Andelman, Persistence length of a strongly charged rodlike polyelectrolyte in the presence of salt, Phys. Rev. E 67 (2003), 011805.
[37] K. Amundson, E. Helfand, X. Quan, S.D. Smith, Alignment of lamellar block copolymer microstructure in an electric field. 1. Alignment kinetics, Macromolecules 26 (1993) 2698–2703.
[38] K. Amundson, E. Helfand, D.D. Davis, X. Quan, S.S. Patel, et al., Effect of an electric field on block copolymer microstructure, Macromolecules 24 (1991) 6546–6548.
[39] M. Ma, Y. Fu, Structural and Mechanical Properties of Ionic Di-block Copolymers via a Molecular Dynamics Approach, Polymers 11 (2019) 1546.
[40] M. Ma, Y. Fu, A Molecular Dynamics Study of the Mechanical Properties of Ionic Copolymers during Tension-Recovery Deformation, Macromol. Theory Simul. n/a (2020), 2000081.
[41] V. Sethuraman, B.H. Nguyen, V. Ganesan, Coarse-graining in simulations of multicomponent polymer systems, J. Chem. Phys. 141 (2014), 244904.
[42] V. Sethuraman, V. Pryamitsyn, V. Ganesan, Normal Modes and Dielectric Spectra of Diblock Copolymers in Lamellar Phases, Macromolecules 49 (2016) 2821–2831.
[43] K.-H. Shen, M. Fan, L.M. Hall, Molecular Dynamics Simulations of Ion-Containing Polymers Using Generic Coarse-Grained Models, Macromolecules 54 (2021) 2031–2052.
[44] K.-H. Shen, L.M. Hall, Effects of Ion Size and Dielectric Constant on Ion Transport and Transference Number in Polymer Electrolytes, Macromolecules 53 (2020) 10086–10096.
[45] T.L. Morkved, M. Lu, A.M. Urbas, E.E. Ehrichs, H.M. Jaeger, et al., Local Control of Microdomain Orientation in Diblock Copolymer Thin Films with Electric Fields, Science 273 (1996) 931.
[46] J.W. Dugger, W. Li, M. Chen, T.E. Long, R.J.L. Welbourn, et al., Nanoscale Resolution of Electric-field Induced Motion in Ionic Diblock Copolymer Thin Films, ACS Appl. Mater. Interfaces 10 (2018) 32678–32687.
[47] R. Ruiz, L. Wan, R. Lopez, T.R. Albrecht, Line Roughness in Lamellae-Forming Block Copolymer Films, Macromolecules 50 (2017) 1037–1046.